

EFFECT OF ASPECT RATIO ON HEAT TRANSFER IN A DIFFERENTIALLY HEATED SQUARE CAVITY USING NON-NEWTONIAN NANOFLUID

Krishanu Sarkar¹ and Apurba Kumar Santra^{2*}

¹*Department of Aerospace Engineering and Applied Mechanics, Bengal Engineering and Science University, Shibpur Howrah-711103, West Bengal, India.*

²*Department of Power Engineering, Jadavpur University, Salt Lake Campus, Block – LB, Plot-8, Sector – III, Salt Lake, Kolkata – 700 098, India.*

*Correspondent author, e_mail: aksantra@pe.jusl.ac.in aksantra@gmail.com

ABSTRACT

Nanofluid is a suspension of solid nanoparticles of metals and their oxides in conventional liquids. It has been considered as a better option due to their improved thermal conductivity. In the present work the effect of aspect ratio (AR) on heat transfer in a differentially heated two-dimensional enclosure has been studied numerically. Copper-water nanofluid has been used and laminar natural convection has been considered. The transport equations have been discretized using finite volume approach and solved using SIMPLER algorithm. Considering the nanofluid to be incompressible and non-Newtonian, the shear stresses have been calculated using Ostwald-de Waele model. The thermal conductivity of the nanofluid has been calculated from the proposed model by Chon *et al.* Study has been conducted for Aspect Ratio=0.125 to 1 while Rayleigh number (Ra) has been varied between 10^5 and 10^7 and solid volume fraction (ϕ) of copper particles varied from 0% to 5%. Prandtl number of water has been considered to be 7.02. Diameter of copper nanoparticles is 25nm. The hot wall and the cold wall are kept at 40°C and 20°C respectively. In general heat transfer decreases with increase in AR and ϕ , but increases with increase in Ra . For a particular value of ϕ maximum heat transfer is obtained between $AR = 0.15-0.25$, $Ra=10^7$.

Keywords: Nanofluid, Heat transfer, Non-Newtonian, Natural Convection, Square Cavity.

1. INTRODUCTION

Due to the low thermal conductivity of conventional fluids like water, Ethylene Glycol (EG), their performance is limited. Nanofluid, which is a suspension of solid nanoparticles of metals and their oxides (1-100nm diameter) in conventional liquids, has been considered as a better option due to their augmented thermal conductivity [1, 2, 3]. Such enhancement depends on shape, size, concentration and thermal properties of the solid nanoparticles. The nanofluid is stable [4], introduce very little pressure drop and it can pass through nano-channels.

Motivated by the intricacies of nanofluids scientists have been conducting experiments to understand the behaviour of such fluids for many years now. Several models have been proposed by researchers to predict the effective thermal conductivity of nanofluid [5, 6, 7, 8, 9, 10], which was proved to be not realistic as the experimental values were much higher than the predicted values. However the models proposed by some researchers [11,12, 13] considering the localized.

Brownian movement of nanoparticles were proved to be more close to the true nature. In such cases a constant comes into existence which can be easily calculated from experiments. Chon *et al.* [14] have provided a correlation based on experimental results, which gives quite accurate value of effective thermal conductivity of Al_2O_3 -water nanofluid. Kebliniski *et al.* [15] have exposed new mechanisms capable of explaining the experimentally enhanced thermal conductivity of nanofluid, these conclusions have been well supported by the result obtained from molecular dynamics (MD simulation).

Complicacy arises while revealing the rheology of the nanofluid. The well-known viscosity model given by Brinkman [16] gives lower value than that observed by experiments. Kwak and Kim [17] have shown experimentally that the viscosity of nanofluid depends on shear rate and there is a rapid increase in zero shear viscosity when ϕ exceeds 0.2%.

Shear thinning behaviour of various nanofluids has been observed by many researchers [18,19]. They have observed that viscosity of nanofluid increases with the increase in concentration when shear rate is low.

A few experiments have been conducted to study natural convective heat transfer using nanofluid inside a cavity [20, 21, 22]. The general observation of these experiments is that the heat transfer decreases when the concentration of nanoparticles in the nanofluid is augmented. It was revealed that the reason behind this is increase in viscosity at low shear rate. Recently Wen and Ding [22] have experimentally observed that for natural convection with the increase in concentration of nanoparticles the convective heat transfer co-efficient decreases. They have also shown that viscosity of this nanofluid increases rapidly with the inclusion of nanoparticles as shear rate decreases. A large number of literature is found regarding natural convection with nanofluid inside a cavity. Khanafer *et al.* [23] have numerically shown that heat transfer increases with the increase in nanoparticle concentration for a particular Grashoff number for copper nanofluid in a square cavity. They had used Wasp model [6] for thermal conductivity. As they had considered the fluid to be Newtonian their observations were contrary to the experimental result. They had considered the thermal dispersion but that consists of an empirical constant, whose value is still unknown. Recently Santra *et al.* [24] have considered the nanofluid as non-Newtonian and have shown that heat transfer decreases with increase in particle concentration for a differentially heated square cavity. This result matches quite well with the experimental observations.

Jou *et al.* [25] have performed the same study [23] to observe the effect of aspect ratio (AR) of the enclosure on heat transfer for Cu-water nanofluid considering ϕ upto 20%. Abunada *et al.* [26] have studied the effect of aspect ratio on heat transfer due to natural convection in a differentially heated cavity using Cu-EG-Water nanofluid. The AR was varied between 0.5 and 2. They have observed that heat transfer decreases with increase in AR.

The study on nanofluid is very much necessary for nanotechnology based cooling applications such as MEMS, including ultrahigh thermal conductivity coolants, lubricants, hydraulic fluids and metal cutting fluids. Due to the fact that under normal condition the natural convection is the only mode of heat transfer, the components may be more prone to damage.

The present paper makes an effort to show the effect of aspect ratio on heat transfer and flow pattern because of laminar natural convection of copper-water nanofluid in a differentially heated cavity. The nanofluid has been considered to be non-Newtonian. The thermal conductivity model proposed by Chon *et al.* [14] has been used to determine the effective thermal conductivity of the nanofluid.

The viscosity of nanofluid has been calculated using Ostwald-de Waele model (two parameter power law model) for a non-Newtonian shear thinning fluid [24]. To the best of the knowledge of the authors, no other numerical study on buoyancy driven heat transfer analysis using nanofluid particularly considering the fluid as non-Newtonian and the aforesaid thermal conductivity model has been reported till the present date. Here the authors have used the primitive variables, instead of stream function & vorticity method [23, 25].

2. MATHEMATICAL FORMULATION

2.1 Problem Statement

The geometry of the present problem is shown in Figure 1. The figure consists of a two-dimensional square enclosure of height h and width l .

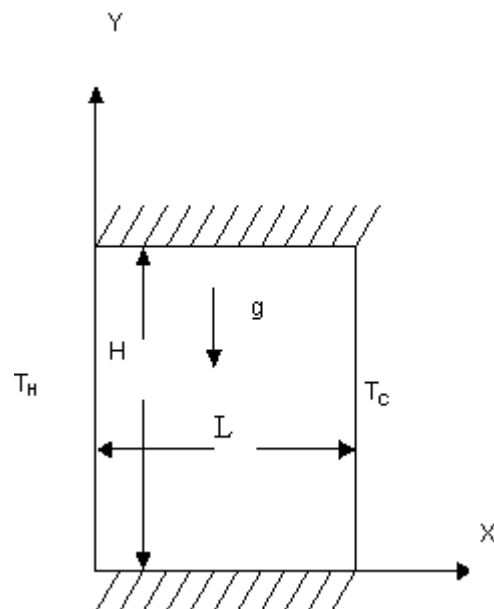


Figure 1: Geometry of the present problem

The temperatures of the two sidewalls of the cavity are maintained at T_H and T_C (reference temperature). The top and the bottom horizontal walls have been considered to be insulated *i.e.*, non-conducting and impermeable to mass transfer. A mixture of water and solid spherical copper particles of 25 nm diameter filled the enclosure is filled. The nanoparticles are considered to be of uniform shape and size. The nanofluid is assumed to be incompressible and non-Newtonian. The flow is laminar. Also it is assumed that the liquid and solid are in thermal equilibrium and they flow at same velocity. All the thermo-physical properties are kept constant except the density, which has been incorporated only in the body force term by employing the Boussinesq approximation.

2.2 Governing Equations and Boundary Conditions

The continuity, momentum and energy equations for a steady, 2D flow of a Fourier constant property fluid have been considered. The dimensionless governing equations for a steady, two-dimensional flow of the homogeneous nanofluid are as follows:

$$\frac{\partial U}{\partial X} + \frac{\partial V}{\partial Y} = 0, \quad (1)$$

$$U \frac{\partial U}{\partial X} + V \frac{\partial U}{\partial Y} = -\frac{\partial P}{\partial X} + \frac{\mu_{app}}{\rho_{nf,0} \alpha_{f,0}} \left[\frac{\partial^2 U}{\partial X^2} + \frac{\partial^2 U}{\partial Y^2} \right] \quad (2)$$

$$U \frac{\partial V}{\partial X} + V \frac{\partial V}{\partial Y} = -\frac{\partial P}{\partial Y} + \quad (3)$$

$$GrPrPr \frac{\rho_{f,0}}{\rho_{nf,0}} (1-\phi + \phi \frac{\rho_s \beta_s}{\rho_f \beta_f}) \theta + \frac{\mu_{app}}{\rho_{nf,0} \alpha_{f,0}} \left[\frac{\partial^2 V}{\partial X^2} + \frac{\partial^2 V}{\partial Y^2} \right] + U \frac{\partial \theta}{\partial X} + V \frac{\partial \theta}{\partial Y} = \frac{k_{nf} (\rho Cp)_{f,0}}{k_f (\rho Cp)_{nf,0}} \left[\frac{\partial^2 \theta}{\partial X^2} + \frac{\partial^2 \theta}{\partial Y^2} \right] \quad (4)$$

Here the apparent viscosity of the nanofluid is

$$\mu_{app} = m \left(\frac{\alpha_{f,0}}{h^2} \right)^{(n-1)} \quad (5)$$

$$\left[2 \left\{ \left(\frac{\partial U}{\partial X} \right)^2 + \left(\frac{\partial V}{\partial Y} \right)^2 \right\} + \left(\frac{\partial V}{\partial X} + \frac{\partial U}{\partial Y} \right)^2 \right]^{\frac{1}{2}} \quad (n-1)$$

The detail of the equations can be obtained from Santra *et al.* [24]

The effective density of the nanofluid at reference temperature is

$$\rho_{nf,0} = (1-\phi)\rho_{f,0} + \phi\rho_{s,0} \quad (6)$$

and the heat capacitance of nanofluid is

$$(\rho Cp)_{nf} = (1-\phi)(\rho Cp)_f + \phi(\rho Cp)_s \quad (7)$$

as given by Xuan *et al.* [3].

Here *m* and *n* are two empirical constants, which depend on the type of nanofluid used. The values of *m* and *n* for different ϕ have been given in Table 1 [24]. It is to be noted that for a shear thinning fluid the value of *n* is less than 1.

The effective thermal conductivity of fluid has been determined by the model proposed by Chon *et al.* [14]. For the two-component entity of spherical-particle suspension the model gives

$$\frac{k_{nf}}{k_f} = 1 + 64.7\phi^{0.7460} \left(\frac{d_f}{d_p} \right)^{0.3690} \quad (8)$$

$$\left(\frac{k_p}{k_f} \right)^{0.7476} Pr^{0.9955} Re^{1.2321}$$

Where $Re = \frac{\rho_f k_b T}{3\pi\mu^2 l_f} \quad (9)$

Here *k_b* is the Boltzmann constant, value of which is 1.3807x10⁻²³ J/K and *l_f* is the mean free path of water, the value of which is 0.17 nm [14]. The calculation of effective thermal conductivity can be obtained from equation (8).

Table1: Values of fluid behaviour index parameters (*m, n*) [24]

Solid Volume Fraction (ϕ) (%)	<i>m</i> (N.sec ⁿ .m ⁻²)	<i>n</i>
0.5	0.00187	0.880
1.0	0.00230	0.830
1.5	0.00283	0.780
2.0	0.00347	0.730
2.5	0.00426	0.680
3.0	0.00535	0.625
3.5	0.00641	0.580
4.0	0.00750	0.540
4.5	0.00876	0.500
5.0	0.01020	0.460

The above equations (1)-(4) has been solved using the following boundary conditions.

$$u = v = \frac{\partial T}{\partial y} = 0 \text{ at } y = 0, h \text{ and } 0 \leq x \leq l ;$$

$$\text{i.e., } U = V = \frac{\partial \theta}{\partial Y} = 0 \text{ at } Y=0,1.0 \text{ and}$$

$$0 \leq X \leq 1.0 .$$

$$T = T_H, u = v = 0 \text{ at } x = 0 \text{ and } 0 \leq y \leq h ;$$

$$\text{i.e., } \theta = 1.0 \text{ and } U = V = 0 \text{ at } X = 0 \text{ and } 0 \leq Y \leq 1.0 .$$

$$T = T_C, u = v = 0 \text{ at } x = l \text{ and } 0 \leq y \leq h ;$$

$$\text{i.e., } \theta = 0 \text{ and } U = V = 0 \text{ at } X = 1.0 \text{ and } 0 \leq Y \leq 1.0 .$$

From the converged solutions, we have calculated *Nu_y* (Local Nusselt number) and \overline{Nu} (Average Nusselt number) for the hot wall as follows

$$Nu_y = -\frac{k_{eff}}{k_f} \frac{\partial \theta}{\partial X} \Big|_{X=0,Y} \quad (10)$$

$$\overline{Nu} = \frac{1}{H} \int_0^H Nu_y \cdot dY \Big|_{x=0} \quad (11)$$

The dimensionless stream function ψ has been defined as $U = \partial\psi/\partial Y$ and $V = -\partial\psi/\partial X$. The stream function at any grid location (*X, Y*) is calculated as

$$\psi(X, Y) = \int_{Y_0}^Y U \cdot \partial Y + \psi(X, Y_0) \quad (12)$$

Along the solid boundary the stream function is taken as zero. $\psi(X, Y_0)$ is known either from the previous calculation, or, from the boundary condition.

3. NUMERICAL APPROACH AND VALIDATION

The governing momentum, mass and energy equations have been discretized by a control volume approach using a power law profile approximation. The computational domain has been divided into 81 X 81 non-uniform grids. A grid independency test has been carried out with $Ra=10^7$, $AR= 2$ and 3 for clear fluid. It is found that increasing grids to 91X91, gives minute change in the average Nusselt Number (below 0.02%).

At the boundaries finer grids have been taken. The set of discretized equations have been solved iteratively, through alternate direction implicit ADI, using the SIMPLER algorithm [27]. For convergence, under-relaxation technique has been employed. To check the convergence, the mass residue of each control volume has been calculated and the maximum value has been used to check the convergence. 10^{-7} was set as the convergence criterion.

The results are validated with the results of de Vahl Davis [28] for different Ra , which has been summarized in Table 2. The difference between the average Nusselt number of de Vahl Davis and that obtained by the present code is well within acceptable limit. Apart from this the average Nusselt number closely matches with that of Santra *et al.* [24] for $AR=1$.

Table 2: Comparison of results for validation

Rayleigh Number (Ra)	\overline{Nu} of de Vahl Davis	\overline{Nu} of present code
10^4	2.243	2.245
10^5	4.519	4.521
10^6	8.799	8.813

4. RESULTS AND DISCUSSION

The effect of aspect ratio (AR) on heat transfer due to laminar natural convection in a differentially heated enclosure has been studied numerically. Water has been considered as the base fluid with $Pr=7.02$ (at $20^\circ C$). Solid spherical nanoparticles of copper of 25nm diameter dispersed in water are considered to be the nanofluid. The effective thermal conductivity of the nanofluid has been calculated from the correlation given by Chon *et al.* [14]. This effective thermal conductivity depends on temperature. The thermal properties as well as the physical properties have been tabulated in Table 3. The values of the constants m and n are summarized in Table 1, to calculate the effective viscosity of the nanofluid.

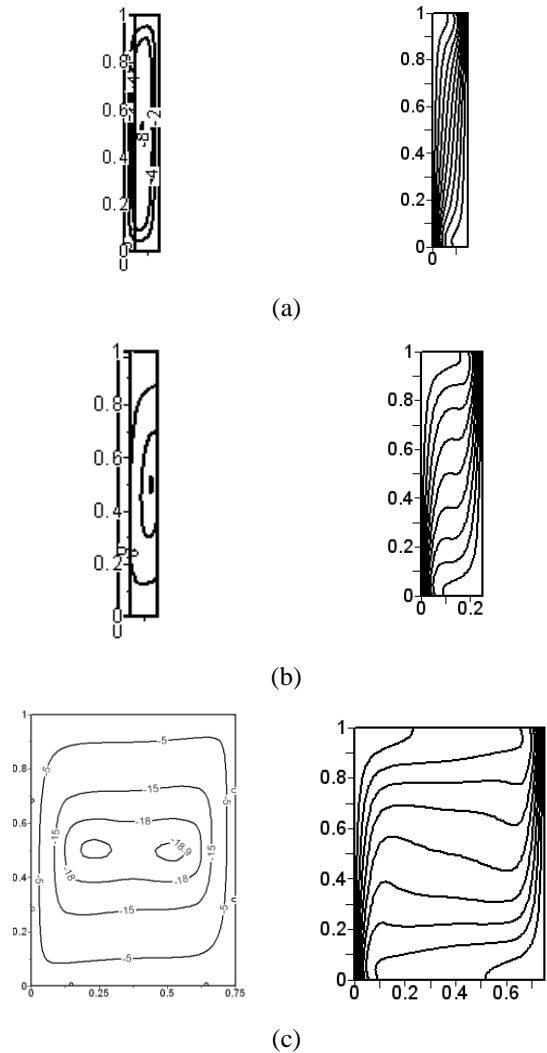
Results are presented for different AR (from 0.125 to 3) while Ra and ϕ have been varied from 10^4 to 10^7 and from 0.0 % to 5.0% (with the increment of 0.5%) respectively. The temperature of the hotter wall is $40^\circ C$ (313K) and that of the cold wall is $20^\circ C$ (293K).

Table 3: Thermophysical properties of different phase at $20^\circ C$

Property	Fluid (water)	Solid (copper)
C_p (J/Kg K)	4181.80	383.1
ρ (Kg/m ³)	1000.52	8954.0
k (W/m K)	0.597	386.0
β (K ⁻¹)	210.0×10^{-6}	51.0×10^{-6}

4.1 Effect of Aspect Ratio on Streamlines and Isotherms

Since the heat transfer depends on the temperature variation within the cavity and the flow pattern, the effect of AR on the streamlines and the isotherms has been shown.



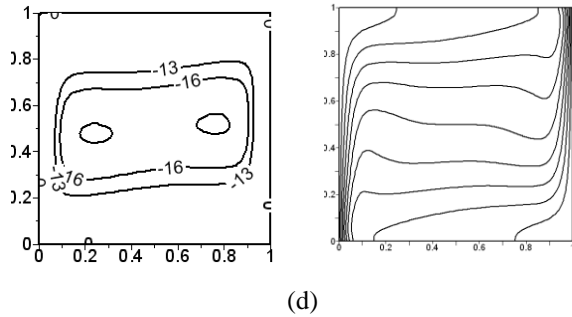


Figure 2: Streamlines and isotherms for $Ra = 10^7$, $\phi = 5\%$ for AR = (a) 0.15, (b) 0.25, (c) 0.75, (d) 1.0

Figure 2 represents the streamlines and isotherms for $Ra=10^7$ for different AR when $\phi=5\%$. From the obtained diagrams of streamlines it is observed that with the increase in AR the dimension of the central cavity of the circulation is increases. The thickness of the velocity boundary layer is increasing as well. It is observed from the figures of streamlines that the maximum value of dimensionless stream function is increasing with the increase in the AR at a very slow rate. When the AR is 1 the maximum value becomes 19. This observation indicates that with the increase in AR the velocity of flow has a tendency to increase.

The diagrams of isotherms show that when the AR is altered the density of isotherms changes. For lower values of AR the isotherms are closely placed and the spacing between isotherms increases with the increase in AR. Also the thickness of the thermal boundary layer is increasing; isothermal stagnant core is also increasing too. This is due to the fact that the width of the cavity increases with the increase in AR. Therefore fluid has to travel a longer distance so the tendency of heat transfer by convection reduces, thus enhancing the probability of heat transfer by conduction.

The obtained patterns of isotherms and streamlines hint at the presence of immobile fluid particles at the centre of the cavity.

4.2 Effect of Nanoparticle Concentration on Streamlines and Isotherms

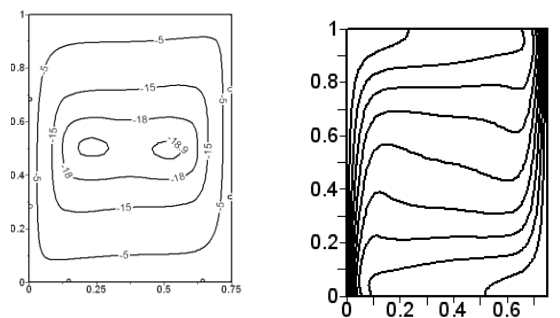
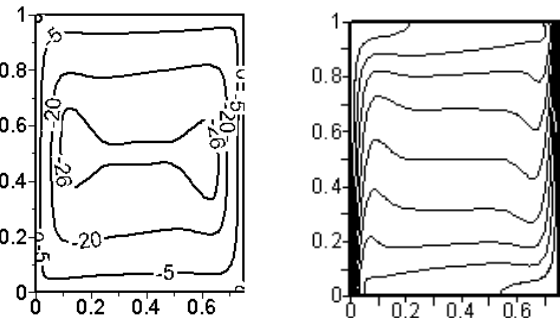
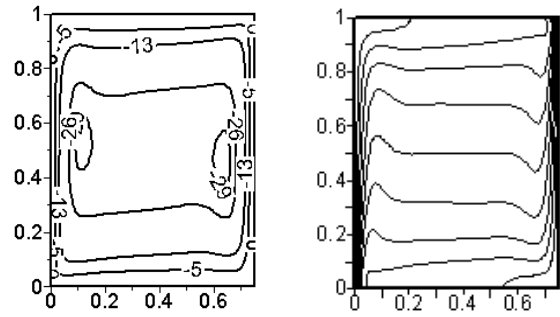
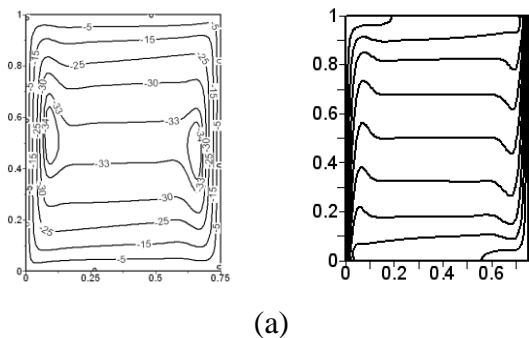
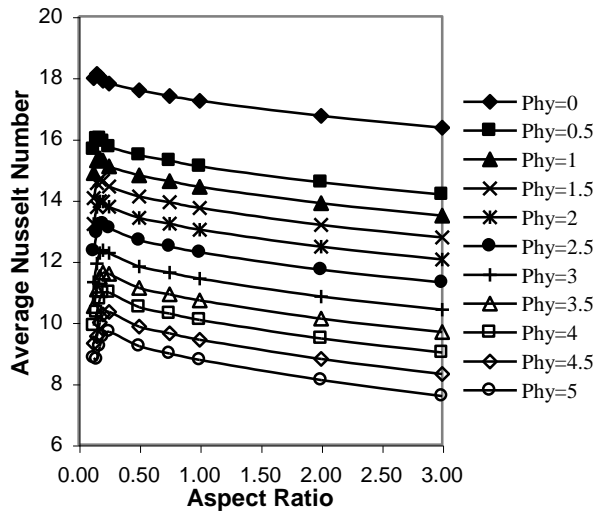
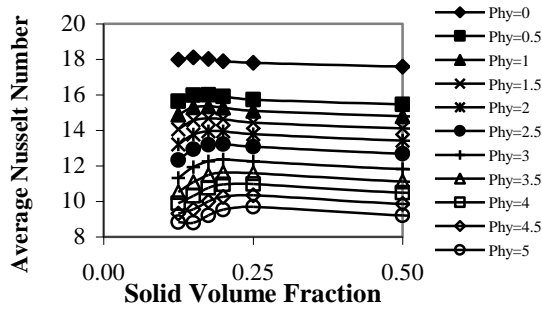


Figure 3: Streamlines and isotherms for $Ra = 10^7$, AR 0.75 for $\phi =$ a) 0%, b) 1%, c) 2%, d) 5%.

Figure 3 depicts the streamlines and isotherms for $\phi = 0\%$ to 5% when $Ra = 10^7$ and AR = 0.75. It is observed that with the increase in concentration of the nanoparticles in the suspension the strength of the circulation decreases. The figures of streamlines at the same time show that the dimension of the core zone is diminishing when the solid volume fraction is enhanced. As the nanofluid is non-Newtonian its viscosity enhances with the increase in nanoparticle concentration. As a result of which the velocity of the nanofluid reduces thus increasing the velocity boundary layer thickness.



(a)



(b)

Figure 4: Variation of average Nusselt number with Aspect Ratio and ϕ for $Ra=10^7$

4.3 Effect of Solid Volume Fraction on Average Nusselt Number

The average Nusselt number for various AR and ϕ has been presented in Fig.4 for $Ra=10^7$

The figure shows that for a particular ϕ the average Nusselt number first increases with increase in AR and after achieving the zenith it decreases gradually. This peak value shifts towards right with increase in nanoparticle concentration. The maximum heat transfer is observed between $AR=0.15$ to 0.25 . The space available for molecular movement increases as AR increases from 0.15 , at the same time the dimension of the central core increases, these two factors play the major role in defining the optimum AR for heat transfer. At $AR=0.15$ the circulation is suppressed as the space for fluid movement is limited. As AR increases this space increases and convection as well as heat transfer increases. After reaching the optimum value, it decreases again as the boundary layer thickness increases with increase in AR as described in Figure 2.

It is also observed that the average Nusselt number decreases for a particular AR with increase in ϕ . It is apparent that the heat transfer should increase with ϕ as effective thermal conductivity of nanofluid increases with ϕ . But here we observe the opposite phenomena as the fluid is non-Newtonian and shows shear-thinning behaviour. Hence the viscosity increases with ϕ , which decrease the convective heat transfer. This can also be explained from Figure 3. As with increase in ϕ the thermal boundary layer thickness increases, the heat transfer decreases. Thus increase in heat transfer due to conduction is nullified. Such observations are similar to the various experimental results [21, 22].

5. CONCLUSIONS

The effect of aspect ratio (AR) on heat transfer has been numerically studied in a differentially heated enclosure where Cu-water nanofluid has been considered. The Rayleigh number and solid volume fraction have been varied from 10^5-10^7 and $0\%-5\%$ respectively. The range of AR used in this case is from 0.125 to 1 . The used nanofluid consists of copper nanoparticles suspended in pure water; the diameter of copper nanoparticles is $25nm$. The Prandtl number of water has been considered to be 7.02 . The hot wall and the cold wall are kept at $40^\circ C$ and $20^\circ C$ respectively. The nanofluid exhibits non-Newtonian behaviour. Shear stress has been calculated using Ostwald-de Waele model. The effective thermal conductivity has been calculated using the model proposed by Chon *et al.*

The results show that with increase in Aspect ratio the heat transfer decreases for a particular solid volume fraction and Rayleigh Number. The trend is slightly different for $Ra=10^7$, where heat transfer first increases and then decreases. For a particular ϕ , the highest value of heat transfer has been observed for $Ra=10^7, AR=0.15-0.25$.

Experiments should be carried out for observing the nature of heat transfer in this type of differentially heated cavities.

REFERENCES

1. Lee S., Choi S.U.S., Li S. and Eastman J. A., Measuring Thermal Conductivity of Fluids Containing Oxide Nanoparticles, Trans ASME J. of Heat Transfer, 121, (1999) 280-289.
2. Eastman J.A., Choi S.U.S., Li S., Yu W. and Thompson L. J., Anomalous Increased Effective Thermal Conductivities of Ethylene Glycol-Based Nanofluids Containing Copper Nanoparticles, Applied Physics Letter, 78, (2001) 718-720.

3. Xuan Y. and Li Q., Heat Transfer Enhancement of Nanofluids, *Int. J. Heat and Fluid Flow*, 21, (2000) 58-64.
4. Zhou D.W., Heat Transfer Enhancement of Copper Nanofluid with Acoustic Cavitation, *Int. J. Heat and Mass Transfer*, 47, (2004) 3109-3117.
5. Hamilton R.L. and Crosser, O.K., Thermal conductivity of heterogeneous two-component systems, I & EC Fundamentals 1, (1962) 182-191.
6. Wasp F.J., Solid-Liquid Flow Slurry Pipeline Transportation. *Trans. Tech. Pub., Berlin*. (1977)
7. Maxwell-Garnett J.C., Colours in metal glasses and in metallic films, *Philos. Trans. Roy. Soc. A* 203, (1904) 385-420.
8. Bruggeman D.A.G., Berechnung Verschiedener Physikalischer Konstanten von Heterogenen Substanzen, I. Dielektrizitätskonstanten und Leitfähigkeiten der Mischkörper aus Isotropen Substanzen. *Annalen der Physik*. Leipzig 24 (1935) 636-679.
9. Wang B. X., Zhou L.P. and Peng X. F., A Fractal Model for Predicting the Effective Thermal Conductivity of Liquid with Suspension of Nanoparticles, *Int. J. Heat and Mass Transfer*, 46, (2003) 2665-2672.
10. Yu W. and Choi S.U.S., the role of interfacial layer in the enhanced thermal conductivity of nanofluids: A renovated Maxwell model, *Journal of Nanoparticles Research*, (2003) 167-171.
11. Kumar D. H., Patel H. E., Kumar V. R. R., Sundararajan T., Pradeep T. and Das S. K., Model for conduction in nanofluids, *Physical Review Letters*, 93 (2004) 144301-1-3
12. Prasher R., Bhattacharya P and Phelan P. E., Brownian- Motion-Based Convective-Conductive Model for the Effective thermal Conductivity of Nanofluid, *ASME Journal of Heat Transfer*, 128 (2006) 588-595.
13. Patel H.E., Sundararajan T, Pradeep T., Dasgupta A., Dasgupta N. and Das S. K., A micro-convection model for thermal conductivity of nanofluid, *Pramana-journal of Physics*, 65 (2005) 863-869.
14. Chon et al *APPLIED PHYSICS LETTERS* 87, 153107 (2005)_
15. Keblinski P., Phillpot S. R., Choi S.U.S. and Eastman J. A., Mechanisms of Heat Flow in Suspensions of Nano-sized Particles (Nanofluids), *Int. J. Heat and Mass Transfer*, 45, (2002) 855-863.
16. Brinkman H.C., The Viscosity of concentrated suspensions and solutions, *J. Chemistry Physics*, 20 (1952) 571-581.
17. Kwak K. and Kim C., Viscosity and thermal conductivity of copper oxide nanofluid dispersed in ethylene glycol, *Korea-Australia Rheology Journal*, 17 (2005) 35-40.
18. Chang H, Jwo C. S., Lo C. H., Tsung T. T., Kao M. J. and Lin H. M., Rheology of CuO nanoparticle suspension prepared by ASNSS, *Rev. Adv. Material Science* 10 (2005) 128-132.
19. Ding Y., Alias H., Wen D. and Williams R. A., Heat transfer of aqueous suspensions of carbon nanotubes ((CNT nanofluids), *Int. J. Heat and Mass Transfer*, 49 (2006) 240-250.
20. Kang C., Okada M., Hattori A. and Oyama K., Natural convection of water-fine particle suspension in a rectangular vessel heated and cooled from opposing vertical walls (classification of the natural convection in the case of suspension with narrow-size distribution), *Int. J. Heat Mass Transfer*, 44 (2001) 2973-2982.
21. Putra N., Roetzel W. and Das S.K., Natural convection of nano-fluids, *Heat and Mass Transfer*, 39 (2003) 775-784.
22. Wen D. and Ding Y., Natural Convective Heat Transfer of Suspensions of Titanium Dioxide Nanoparticles (Nanofluids), *IEEE TRANSACTIONS ON NANOTECHNOLOGY*, 5 (2006) 220-227.
23. Khanafer K., Vafai K. and Lightstone M., Buoyancy-driven Heat Transfer Enhancement in a Two-dimensional Enclosure Utilizing Nanofluids, *Int. J. Heat and Mass Transfer*, 46 (2003) 3639-3653.
24. Santra A. K., Sen S. and Chakraborty Niladri, Study of Heat Transfer Augmentation in a Differentially Heated Square Cavity Using Copper-Water Nanofluid, *International Journal of thermal Sciences*, 47 (2008), 1113-1122.
25. Jou R.Y. and Tzeng S. C., Numerical research of nature convective heat transfer enhancement filled with nanofluids in rectangular enclosures, *International Communications in Heat and Mass Transfer*, 33 (2006) 727-736.
26. Abunada E. and Chakma A. J., Effect of nanofluid variable properties on natural convection in enclosures filled with a CuO-EG-Water nanofluid, *Int. J. Thermal Sciences*, 49 (2010) 2339-2352
27. Patankar S.V, *Numerical Heat Transfer and Fluid Flow*, Hemisphere, Washington D. C., (1980).
28. de Vahl Davis G., Natural Convection of Air in a Square Cavity, a Benchmark Numerical Solution, *Int. J. Numer. Methods Fluids*, 3 (1962) 249-264.

NOMENCLATURE

Symbol

AR	Aspect Ratio (l/h)	
c	specific heat	(J/kg K)
d	diameter	
Gr	Grashoff number	
g	acceleration due to gravity	(m/s^2)
H, L	dimensionless cavity height and dimensionless width of cavity	
h, l	dimensional height and width of cavity	(m)
k	thermal conductivity	(W/mK)
k_b	Boltzmann constant	
k_{eff}	effective thermal conductivity	
l_f	mean free path of water	
m, n	the respective consistency and fluid behaviour index parameters,	
$\frac{Nu_y}{Nu}$	local Nusselt number of the heater average Nusselt number at the heater	
P	pressure	(N/m^2)
p	dimensionless pressure ($p-p_0$) $H^2/\rho_0\alpha^2$	
Pr	Prandtl number of fluid, ν_f / α_f	
Ra	Rayleigh Number, $Gr Pr$	
Re	Reynolds number	
T	temperature	(K)
T_H, T_C	temperature of the heat source and sink respectively	(K)
u, v	velocity components in the x and y directions respectively	(m/s)
U, V	dimensionless velocities ($U=uH/\alpha$, $V=vH/\alpha$)	
x, y	horizontal and vertical coordinates respectively	(m)
X, Y	dimensionless horizontal and vertical coordinates respectively ($X=x/h$, $Y=y/h$)	

Greek Symbols

α	thermal diffusivity of the fluid	(m^2/s)
β	isobaric expansion coefficient	(K^{-1})
ϕ	solid volume fraction	
μ	dynamic viscosity	($N.s/m^2$)
ν	kinematic viscosity	(m^2/s)
ρ	density of the fluid	(kg/m^3)
θ	dimensionless temperature ($(T-T_0)/(T_H-T_C)$)	
ψ	dimensionless stream function	
τ	the stress tensor,	
\bullet	the symmetric rate of deformation tensor,	
γ	tensor,	

Subscripts

app	apparent
eff	effective
f	fluid
nf	nanofluid
o	at reference state
p	particle
s	solid

AUTHOR BIOGRAPHY



Mr. Krishanu Sarkar is a Post Graduate student in the Department of Aerospace Engineering and Applied Mechanics at Bengal Engineering And Science University, Shibpur, India. He has research interest in nanofluid and heat transfer. etc. He has one publications in an international peer reviewed journal.



Dr. Apurba K. Santra is an Associate Professor at Department of Power Engineering at Jadavpur University, Kolkata, India. He has 13 years of teaching experience and 7 years of industry experience. He has research interest in heat transfer using nanofluid, MHD power generation, engine combustion etc. He has 11 publications in various national and international journals.